


Cite this: *RSC Adv.*, 2023, 13, 7789

Performance of a membrane fabricated from high-density polyethylene waste for dye separation in water

Utari Zulfiani,^a Afdhal Junaidi,^a Cininta Nareswari,^a Badrut Tamam Ibnu Ali,^a Juhana Jaafar,^b Alvin Rahmad Widyanto,^a Saiful,^c Hadi Nugraha Cipta Dharma^b and Nurul Widiastuti^{id} *^a

Industrial growth can have a good impact on a country's economic growth, but it can also cause environmental problems, including water pollution. About 80% of industrial wastewater is discharged into the environment without treatment, of which 17–20% is dominated by dyes, such as methylene blue (MB) and methyl orange (MO) from the textile industry. Only about 5% of a textile dye is used in the dyeing process and the rest is discarded. This problem, of course, requires special handling considering the harmful effects to health. On the other hand, the abundance of plastic waste is increasing by 14% or 85 000 tons per year. This problem must be solved due to its film-forming properties. High-density polyethylene (HDPE) is one type of plastic used as a membrane material. Therefore, in this study, HDPE plastic waste was utilized as a membrane for dye removal. In this study, HDPE plastic waste was fabricated via a thermal-induced phase-separation method using mineral oil as a solvent at various concentrations of 8%, 10%, 13%, and 15% (w/w). All the membranes were characterized by scanning electron microscopy, Fourier transform infrared spectroscopy, and contact angle measurements. The results showed that the HDPE membrane at a concentration of 15% displayed the best performance compared to the others in terms of MB rejection. The negative charge (−36.9) of the HDPE membrane was more effective for cationic dye removal compared to the anionic dye. The flux and rejection of HDPE 15% for 100 ppm MB and MO removal were 2.71 and 4.93 L m^{−2} h^{−1}, and 99.72% and 89.8%, respectively. The pure water flux of the membrane was 15.01 L m^{−2} h^{−1} and the tensile strength was 0.3435 MPa.

Received 29th November 2022

Accepted 12th January 2023

DOI: 10.1039/d2ra07595d

rsc.li/rsc-advances

1 Introduction

The abundance of plastic waste poses a problem that requires serious attention. Its fabrication for various uses makes it not easily decomposed, causing its abundance to increase.¹ This situation was exacerbated by the COVID-19 pandemic, where the demand for single-use plastic continued to increase but without additional handling for its disposal. As a result, 8.4 ± 1.4 million tons of plastic waste were produced from 193 countries, of which it was estimated that 25.9 ± 3.8 thousand tons of this waste was dumped into the global oceans and about 72% of this waste came from Asia.² In 2022, based on Indonesia waste management information data, plastic is ranked second after food waste and accounts for around 17.47% of the total

waste. Hidayat *et al.*¹ reported that the use of plastic in Indonesia reaches 85 000 tons annually and as many as 3.2 million tons are dumped into the sea, this ranks Indonesia as the second worst country in the world in terms of poor waste management after China.³

Besides the problem of plastic waste, the issue of clean water is taking center stage in various countries due to the increase in population and industrial growth.⁴ Zhang *et al.*⁵ estimated that approximately 1.84 × 10¹⁰ m³ of dye wastewater is produced from industries. Some industries that produce dye waste with high concentrations include dye manufacture, tanning and painting, paper and pulp, dyes, and textile. The highest percentage of dye waste disposal is textile.⁶ There are about 100 000 types of dyes with a total annual production of 7 × 10⁵ tons.⁷ The textile industry produces about 15% or 1000 tons of waste annually with a concentration of 5–1500 ppm that is discharged into aquatic waters.^{7,8}

Dyes, even in low concentration (<1 ppm), can be visually detected due to their high visibility and can affect aquatic life and so are not only aesthetically displeasing but also toxicologically harmful.^{7,9,10} Azo-derived dyes account for about 70% of the total world dye production.¹¹ Among all the tested dyes,

^aDepartment of Chemistry, Faculty of Science and Data Analytics, Institut Teknologi Sepuluh Nopember, Sukolilo, Surabaya 60111, Indonesia. E-mail: nurul_widiastuti@chem.its.ac.id

^bAdvanced Membrane Technology Research Centre (AMTEC), Universiti Teknologi Malaysia, 81310 Skudai, Johor Bahru, Malaysia

^cDepartment of Chemistry, Faculty of Mathematic and Natural Science, Universitas Syiah Kuala, Banda, Aceh 23111, Indonesia



The solvent factor also determines the performance of HDPE membranes. Shokri *et al.*²⁹ reported that HDPE had poor compatibility with several types of solvents and additives, which would impact the performance of the resulting membrane.

The membrane was fabricated by thermally induced phase separation (TIPS) using the method of Shokri *et al.*²⁹ with several modifications. HDPE plastic was dissolved in mineral oil at

various polymer concentrations of 8%, 10%, 13%, and 15% (w/w), the proportions are listed in Table 1. The mixture was homogenized at a temperature of 140 °C with a rotation of 100 rpm for 2 h and left for 30 min to remove the gases. The homogeneous solution was then poured and cast on a glass sheet that had been heated. The glass plate was immediately quenched in a water bath to induce phase separation. After peeling off the plates, the membranes were immersed in acetone for 24 h to extract the mineral oil and dried at room temperature.²⁹ The preparation scheme is shown in Fig. 1.

2.3 Membrane characterizations

The morphology of the cross-sectional and the surface of the HDPE membrane were analyzed by scanning electron microscopy (SEM) with energy dispersive X-ray spectroscopy (EDX, Zeis Evo MA 10 and Hitachi flex SEM 100) with an accelerating voltage of 20.0 kV. For the cross-section imaging, the membranes were cut inside a flow of liquid nitrogen to obtain a smooth cross-section of the surface. Then, the membranes were coated with a thin layer of gold and inserted into the specimen chamber for analysis of the morphological structure.³⁵ SEM in this research was used to study the effect of the polymer concentration on the pore structure in the membranes. The average pore size on the membrane was measured using ImageJ software. The porosity of the membrane was measured with Archimedes method. The membrane was cut to a specific size (0.005 m²) and dried in an oven at 110 °C for 30 min before soaking for 24 h in isobutanol. The wet membrane was then weighed. The porosity was calculated by eqn (1), where ε is the porosity (%); W_1 is the mass of the wet sample (g); W_2 is the mass of the dry sample (g); ρ_1 is the density of HDPE (0.941 g cm⁻³); and ρ_2 is the density of isobutanol (0.802 g cm⁻³):³⁰

$$\varepsilon (\%) = \frac{(W_1 - W_2)/\rho_1}{\frac{W_1 - W_2}{\rho_1} + (W_2/\rho_2)} \times 100 \quad (1)$$

Fourier transform infrared spectroscopy (FTIR, Thermo Scientific Nicolet iS10) was used to determine the functional groups on the membrane. The membrane was cut to a size of 1 × 1 cm and inserted in a sample holder for analysis using infrared (IR) rays in the wavenumber range of 400–4000 cm⁻¹.²⁵

The hydrophobicity of the HDPE membrane was investigated by measuring the contact angle using a 3D optical microscope (3D OM, vhx-5000) at room temperature with 3 L of deionized water as the probe solvent. The surface charge of the membrane was tested by measuring the zeta potential using a Melvern Zetasizer Nano ZS. The mechanical properties of the



Fig. 1 Preparation scheme of the HDPE membrane.

membranes were measured by dynamic mechanical analysis (DMA, SDTA861, Mettler) with the force ranging from 0.01 to 1 N. The tensile strength of membrane was calculated with eqn (2), where τ is the tensile strength (MPa), F_{\max} is the maximum strength load (N), and A is the membrane area (m²):

$$\tau = \frac{F_{\max}}{A} \quad (2)$$

Meanwhile, the elongation at break was calculated with eqn (3), where ε is the elongation (%), d is the length at break (mm), and a is the initial length (mm):

$$\varepsilon = \frac{d - a}{a} \times 100\% \quad (3)$$

2.4 Membrane performance

Water flux and dye rejection tests were performed using a crossflow reactor (Sartorius, viva flow 50R) with an effective membrane area of 50 cm². In this system, the flow rate of the feed flow solution was 100 mL min⁻¹. The membrane flux was calculated with eqn (4),³⁶ where J , V , A , and t are the permeate (L m⁻² h⁻¹), permeate mass (m), membrane surface area (m²), and permeation time (h).

$$J = \frac{m}{A \times t} \quad (4)$$

The rejection of dye was measured using eqn (5),³⁶ where CP and CF are the permeate and feed concentrations of dyes. The concentration of dye was measured using a UV-752N UV-Vis spectrophotometer.

$$R (\%) = \left(1 - \frac{C_P}{C_F}\right) \times 100 \quad (5)$$

Table 1 Proportions of the initial materials used to prepare the HDPE membrane

Membrane (% w/w)	HDPE (g)	Mineral oil (g)
R-HDPE 8%	4	46
R-HDPE 10%	5	45
R-HDPE 13%	6.5	43.5
R-HDPE 15%	7.5	42.5

3 Result and discussion

3.1 Solvent selection

The challenge of using HDPE plastic as a membrane material is due to its resistance to various types of solvents.³⁷ In the process of membrane formation through TIPS, the polymer must



Types of solvents	DMF	DMSO	Toluene	Xylene	Phenol	Cooking oil	<i>n</i> -Hexane	Mineral oil	NMP
Result	Insoluble	Insoluble	Soluble	Soluble	Insoluble	Partially soluble	Insoluble	Soluble	Insoluble
Dielectric constant (ϵ)	38.3	47.2	2.4	2.37	15	3.23	1.88	2.1	32.16
Refractive index	1.430	1.479	1.497	1.5	2.37	1.44	1.38	1.48	2.15

© 2023 The Author(s). Published by the Royal Society of Chemistry

consisted only of a hydrocarbon structure and no other additives, such as talc or CaCO_3 , were detected. The results from the HDPE spectra in this study were in accordance with commercial HDPE spectra based on this theory, namely stretching CH_2 at $2950\text{--}2850\text{ cm}^{-1}$; bending vibration CH_2 at $1470\text{--}1460\text{ cm}^{-1}$; and rocking vibrations of CH_2 at $730\text{--}700\text{ cm}^{-1}$.⁴⁴

3.3 Morphology of the membrane

The surface and cross-sectional morphology of the membranes were analyzed using SEM. The results of the SEM cross-sections of the HDPE membranes showed that the pores of the HDPE membranes were 8% wider than those of the 10%, 13%, and 15% HDPE membranes (Fig. 3). The narrower pore sizes in the R-HDPE 10% and 15% were due to the increase in polymer used in the membrane fabrication. The smallest pore size was for membrane R-HDPE 15%, but between R-HDPE 8% and 10% did not show a significant difference because the concentration in the membrane was almost the same (Fig. 4).

Ajari *et al.*³⁰ also reported that increasing the polymer concentration in polyethylene membranes decreased the porosity of the membranes due to a decrease in the coagulation rate due to the increased polymer concentration. The formation of the membrane morphology is also influenced by the membrane fabrication method, which in this study used the TIPS method. Pore formation in this method occurred after soaking the membrane in the extractant, namely acetone.⁴⁵ The membranes exhibited cellular-like pores, which are the typical



Fig. 3 Cross-sections of the HDPE membranes: (a) R-HDPE 8%, (b) R-HDPE 10%, (c) R-HDPE 13%, and (d) R-HDPE 15%.



Fig. 4 Surfaces of the HDPE membranes: (a) R-HDPE 8%, (b) R-HDPE 10%, (c) R-HDPE 13%, and (d) R-HDPE 15%.

structures that result from the thermally induced phase-separation method.⁴⁶

For all the cases, the pore sizes at the surfaces of the membranes were smaller than the interior pore sizes (Table 3). The smaller pores at the surfaces may be attributed to the higher cooling rate in the surface layers brought about by the contact with water, whereby there would be less time for the formed droplets to coarsen in the surface layers in cooling process. As summarized in Table 3, the porosity of the membranes varied in a small range and showed a slight decreasing tendency with the increase in the total polymer concentration. This may be associated with the reduced volume fraction of the polymer-poor phase in the high polymer concentration case.

3.4 Contact angle

The contact angle is a parameter that determines the hydrophilicity properties of a membrane. Fig. 5 shows the change in

Table 3 Pore sizes and porosities of the membranes

Membrane	Pore size area (μm^2)		Average pore size (μm)		Porosity (%)
	Interior	Surface	Interior	Surface	
R-HDPE 8%	34.744	9.884	5.729	3.637	50.1
R-HDPE 10%	19.928	5.812	3.570	2.579	42.9
R-HDPE 13%	6.955	4.850	2.053	2.138	36.1
R-HDPE 15%	3.683	1.241	1.505	0.950	25.5





Fig. 5 Contact angles of the membranes.

contact angle in the fabricated HDPE membranes. The increase in concentration resulted in membranes with a contact angle greater than 90° . Thus, the membrane could be categorized as hydrophobic.⁴⁷ An increased contact angle with increased concentration is generally associated with the roughness of the membrane surface. The increase in concentration affected the roughness on the surface, causing the hydrophilicity properties of the membrane to decrease. Ajari *et al.*³⁰ reported the same thing in LDPE membranes, where an increase in polymer concentration from 5% to 10% led to an increase in the contact angle of the membrane due to increasing the roughness of the membrane surface.

3.5 Mechanical strength

The mechanical strength of a membrane can be determined by the tensile strength and the elongation. In this research, testing was carried out on the membranes with the lowest concentration, namely R-HDPE 8%, and the highest concentration, namely R-HDPE 15%. Fig. 6 shows the stress-strain curves of the tensile strength of HDPE membranes.

Based on the stress-strain curves, the tensile strength, elongation, and Young's modulus of R-HDPE 8% were 0.0184 MPa, 18.03%, and 4 MPa, respectively. The R-HDPE 15% membrane, which was the highest concentration of polymer

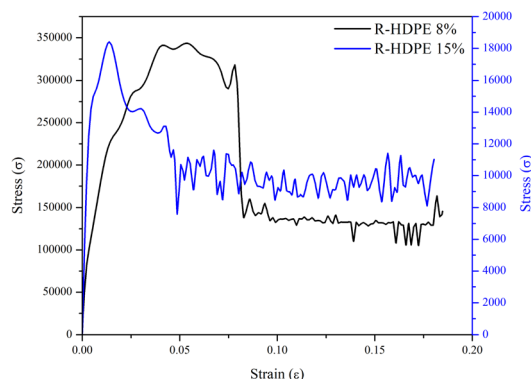


Fig. 6 Stress-strain curves of the HDPE membranes.



Fig. 7 Water flux, MB flux, and MB rejection rates of the HDPE membranes.

tested here, had tensile strength, elongation, and Young's modulus values of 0.3435 MPa, 18.47%, and 40 MPa, respectively. Based on the tensile strength tests, the membrane with a concentration of 15% was stronger than the membrane with a concentration of 8%. This suggests that the increase in the polymer concentration had an impact on the strength of the membrane.

3.6 Membrane performance tests

The membrane performance was tested, including the water flux, MB flux, and MB rejection (Fig. 7). The results obtained showed that the R-HDPE 8% membrane had a water flux of $56.2 \text{ L m}^{-2} \text{ h}^{-1}$, MB flux of $29.8 \text{ L m}^{-2} \text{ h}^{-1}$, and rejection rate of 54.73%; while the R-HDPE 10% membrane had a water flux of $24.43 \text{ L m}^{-2} \text{ h}^{-1}$, MB flux of $14.97 \text{ L m}^{-2} \text{ h}^{-1}$, and rejection rate of 71.09%, and the R-HDPE 13% membrane had a water flux of $18.75 \text{ L m}^{-2} \text{ h}^{-1}$, MB flux of $12.48 \text{ L m}^{-2} \text{ h}^{-1}$, and MB rejection rate of 88.69%. The highest rejection results were found in R-HDPE 15%, namely 98.33%; but this membrane had the lowest water flux and MB flux, which were $15.01 \text{ L m}^{-2} \text{ h}^{-1}$, respectively. The MB flux values on the R-HDPE 8% and R-HDPE 10% membranes were higher than those of the R-HDPE



Fig. 8 R-HDPE 15% performance in the 60 min test with crossflow.



Fig. 9 Performance of the R-HDPE 15% membrane for MO and MB removal.



Fig. 10 Dye removal scheme.

15% membrane, but the rejection values of the R-HDPE 8% and R-HDPE 10% membranes were lower than the rejection value of the R-HDPE 15% membrane. This shows that the polymer concentration affected the pore density of the membrane, whereby the membranes with a higher concentration had smaller pores, which led to a higher rejection of MB.³⁰ The same result was also reported by Othman *et al.*,⁴⁸ namely that polypropylene membranes with a concentration of 20% had smaller pore sizes than membranes with a concentration of 15%, *i.e.* 11.5 vs. 9.01 μm . In an LDPE (low density polyethylene) membrane, the water flux in the membrane with a concentration of 10% also had a lower flux value than that of a 5% LDPE membrane, *i.e.* 0.7 vs. 1.5 $\text{L m}^{-2} \text{h}^{-1}$.³⁰

The test results reported in Fig. 7 are the average flux and membrane rejection rates carried out for 30 min using 10 ppm MB. Based on this test, the R-HDPE 15% membrane showed the best performance with a higher rejection rate than the other membranes. Therefore, the test on the R-HDPE 15% membrane was continued for 90 min to determine the durability of the membrane. Based on Fig. 8, there was an increase in rejection from 5 to 40 min, then at 45 to 60 min, the rejection rate became more stable. At 60 min, the flux and rejection rate of 4.99 $\text{L m}^{-2} \text{h}^{-1}$ and 99.69% were obtained. The test was then continued for 30 min with the same membrane without washing and the flux and rejection were then 3.6 $\text{L m}^{-2} \text{h}^{-1}$ and 99.75%. In general, there was no significant change in the membrane rejection value, but in terms of the flux, there was a significant decrease at 30, 60, and 90 min of the test, namely 9.25, 6.14, and 3.6 $\text{L m}^{-2} \text{h}^{-1}$, respectively.

As indicated by the results in Fig. 8 and 9, the rejection increased with increasing the filtration time and dye concentration. This was because as the feed concentration increased, more dye particles would be collected on the surface of the membrane, which increased the fouling, and thereby reduced

Table 4 Comparison of HDPE membranes fabricated from waste and commercial membranes

Membrane	Contaminant	Rejection (%)	Ref.
HDPE	MB 10 ppm	98.33	This research
	MB 50 ppm	99.27	
	MB 100 ppm	99.72	
	MO 10 ppm	83.64	
	MO 50 ppm	88	
	MO 100 ppm	89.8	
HDPE	River turbidity	12–35	Zukimin <i>et al.</i> ²⁷
PES/HDPE/LDPE/kaolin	Cd 50 ppm	69.3	Mubarak <i>et al.</i> ²⁸
	Pb 50 ppm	76.2	
	Cu 50 ppm	82.5	
HDPE ^a	Humic acid	89.54	Akbari <i>et al.</i> ²⁵
HDPE ^a	BSA	68	Shokri <i>et al.</i> ²⁹
HDPE/EVA ^a	Salt	99.9	Tang <i>et al.</i> ⁵¹
PPSU ^a	Drupel black NT 50 ppm	85	Ghadhban <i>et al.</i> ⁵²
Bentonite ^a	MB 20 ppm	78	Bouazizi <i>et al.</i> ⁵³
	DR 80 20 ppm	99	Daraei <i>et al.</i> ⁵⁴
	AO 74 20 ppm	83	Fradj <i>et al.</i> ⁵⁵
	MB 1 ppm	85	
PVDF/chitosan/clay ^a	MO 32,7 ppm	86	
PAA ^a	Toluidine blue 27 ppm	89	

^a Commercial membranes.

the flux and increased the percentage of dye rejection. On the other hand, the average percentage of dye rejection increased as the time filtration increased.⁴⁹

Fig. 9 shows the performance of the R-HDPE 15% membranes on the separation of MB and MO dye with several concentrations. Based on the rejection data, the R-HDPE 15% membranes had a higher percentage of rejection in MB separation than for MO. MB is cationic, while MO is an anionic dye. Based on the potential zeta measurements, HDPE had a negative charge of -36.9 with water dispersions; thus MB had a high rejection percentage due to the strong electrostatic interaction between the positive charge of the MB dye and negative charge of the R-HDPE 15% membrane. MO filtration showed lower rejection rates than MB, while MO is an anionic dye, thus improving the repulsive force between the dye molecules and membrane surface. This phenomenon is described in Fig. 10. Gnanasekaran *et al.*⁵⁰ also reported that incorporating MIL-100 (Fe) into chitosan led to a high rejection of MB due to the negative charge of the membrane. Based on comparisons with HDPE waste membranes from previous reported studies and commercial HDPE in Table 4, the membranes in this study showed higher rejection of the dyes.

4 Conclusions

HDPE plastic waste can be used as a membrane material to remove MB and MO from water. By comparing the use of commercial HDPE and plastic HDPE for membrane manufacture, the results showed that the concentration of commercial HDPE required was higher, namely 20% w/w, compared to HDPE plastic waste (15% w/w). Both HDPE membranes were made using the TIPS method with mineral oil solvents, resulting in low solvent costs. Due to its negative charge, this membrane was effective for rejecting dye stuffs with positive charge, such as MB, with a rejection of up to 99.72% at an initial MB concentration of 100 ppm. On the other hand, for anionic dyes, such as MO, the percentage rejection was lower at up to 89.8% with the same concentration. Based on the research, membranes with a composition of 15% were more effective in removing MB and MO than the other membranes. Higher polymer concentrations resulted in better rejection results, but lower flux yields. The low flux value produced in the membrane with a concentration of 15% was due to the denser pore size as a result of the addition of the polymer.

Author contributions

Utari Zulfiani: conceptualization, investigation, resources, methodology, and writing – original draft. Afdhal Junaidi and Cininta Nareswari: review & editing. Badrut Tamam Ibnu Ali: conceptualization and methodology. Nurul Widiastuti: conceptualization, supervision, review & editing. Saiful: supervision, review and editing. Juhana Jaafar: supervision and resources, and formal analysis. Alvin Rahmad Widyanto: conceptualization, review – editing and visualization. Hadi Nugraha Cipta Dharma: formal analysis.

Conflicts of interest

There are no conflicts to declare.

Acknowledgements

The authors would like to appreciate the research funding provided by the Ministry of Education and Culture Republic of Indonesia under *Penelitian Magister Menuju Doktor Sarjana Unggul*, Contract number: 1478/PKS/ITS/2022.

References

- 1 Y. A. Hidayat, S. Kiranamahsa and M. A. Zamal, *AIMS Energy*, 2019, 7, 350–370, DOI: [10.3934/ENERGY.2019.3.350](#).
- 2 Y. Peng, P. Wu, A. T. Schartup and Y. Zhang, *Proc. Natl. Acad. Sci. U. S. A.*, 2021, 118(47), 1–6, DOI: [10.1073/pnas.2111530118](#).
- 3 R. Jambeck Jenna, G. Roland, W. Chris, R. Siegler Theodore, P. Miriam, A. Anthony, N. Ramani and L. K. Lavender, *Science*, 2015, 347, 768–770, DOI: [10.1126/science.1260352](#).
- 4 M. M. A. Shirazi, A. Kargari and M. J. A. Shirazi, *Desalin. Water Treat.*, 2012, 49, 368–375, DOI: [10.1080/19443994.2012.719466](#).
- 5 Y. Zhang, W. Cao, B. Zhu, J. Cai, X. Li, J. Liu, Z. Chen, M. Li and L. Zhang, *J. Colloid Interface Sci.*, 2022, 611, 706–717, DOI: [10.1016/j.jcis.2021.12.073](#).
- 6 I. I. Khan, K. Saeed, I. Zekker, B. Zhang, A. H. Hendi, A. Ahmad, S. Ahmad, N. Zada, H. Ahmad, L. A. Shah, T. Shah and I. I. Khan, *Water*, 2022, 14, 242, DOI: [10.3390/w14020242](#).
- 7 A. Ajmal, I. Majeed, R. N. Malik, H. Idriss and M. A. Nadeem, *RSC Adv.*, 2014, 4, 37003–37026, DOI: [10.1039/c4ra06658h](#).
- 8 S. Rafiqat, N. Ali, C. Torres and B. Rittmann, *RSC Adv.*, 2022, 12, 17104–17137, DOI: [10.1039/d2ra01831d](#).
- 9 G. Muthuraman, T. T. Teng, C. P. Leh and I. Norli, *J. Hazard. Mater.*, 2009, 163, 363–369, DOI: [10.1016/j.jhazmat.2008.06.122](#).
- 10 J. Fito, S. Abraham and K. Angassa, *Int. J. Environ. Res.*, 2020, 14, 501–511, DOI: [10.1007/s41742-020-00273-2](#).
- 11 A. A. Setyo Purnomo, *Biodegradasi Metilen Biru*, Deepublish Publisher, Surabaya, 2021.
- 12 E. Oyarce, K. Roa, A. Boulett, S. Sotelo, P. Cantero-López, J. Sánchez and B. L. Rivas, *Polymers*, 2021, 13(19), 3450, DOI: [10.3390/polym13193450](#).
- 13 P. K. Gillman, *Anaesthesia*, 2006, 61, 1013–1014, DOI: [10.1111/j.1365-2044.2006.04808.x](#).
- 14 N. W. Yuningrat, N. Retug and I. M. Gunamantha, *J. Sci. Technol.*, 2016, 5, 692–701, DOI: [10.23887/jst-undiksha.v5i1.8275](#).
- 15 K. O. Iwuzor, J. O. Ighalo, E. C. Emenike, L. A. Ogunfowora and C. A. Igwegbe, *Curr. Res. Green Sustainable Chem.*, 2021, 4, 100179, DOI: [10.1016/j.crgsc.2021.100179](#).
- 16 N. Widiastuti, A. R. Widyanto, I. S. Caralin, T. Gunawan, R. Wijiyanti, W. N. Wan Salleh, A. F. Ismail, M. Nomura and K. Suzuki, *ACS Omega*, 2021, 6, 15637–15650, DOI: [10.1021/acsomega.1c00512](#).



